

Quantitative determination of the critical points of Mott metal-insulator transition in strongly correlated systems

Yuekun Niu(牛月坤), Yu Ni(倪煜), Jianli Wang(王建利), Leiming Chen(陈雷鸣), Ye Xing(邢晔), Yun Song(宋筠), and Shiping Feng(冯世平)

Citation: Chin. Phys. B, 2024, 33 (**1**): 017102. DOI: 10.1088/1674-1056/ad0719
Journal homepage: http://cpb.iphy.ac.cn; http://iopscience.iop.org/cpb

What follows is a list of articles you may be interested in

Quantum phase transitions in CePdAl probed by ultrasonic and thermoelectric measurements

Hengcan Zhao(赵恒灿), Meng Lyu(吕孟), Jiahao Zhang(张佳浩), Shuai Zhang(张帅), and Peijie Sun(孙培杰)
Chin. Phys. B, 2022, 31 (**11**): 117103. DOI: 10.1088/1674-1056/ac8345

$CeAu_2In_4$: A candidate of quasi-one-dimensional antiferromagnetic Kondo lattice

Meng Lyu(吕孟), Hengcan Zhao(赵恒灿), Jiahao Zhang(张佳浩), Zhen Wang(王振), Shuai Zhang(张帅), and Peijie Sun(孙培杰)
Chin. Phys. B, 2021, 30 (**8**): 087101. DOI: 10.1088/1674-1056/ac0a60

Lifshitz transition in triangular lattice Kondo-Heisenberg model

Lan Zhang(张欄), Yin Zhong(钟寅), Hong-Gang Luo(罗洪刚)
Chin. Phys. B, 2020, 29 (**7**): 077102. DOI: 10.1088/1674-1056/ab8da4

Density wave and topological superconductivity in the magic-angle-twisted bilayer-graphene

Ming Zhang(张铭), Yu Zhang(张渝), Chen Lu(卢晨), Wei-Qiang Chen(陈伟强), and Fan Yang(杨帆)
Chin. Phys. B, 2020, 29 (**12**): 127102. DOI: 10.1088/1674-1056/abc7b5

Phase diagram, correlations, and quantum critical point in the periodic Anderson model

Jian-Wei Yang(杨建伟), Qiao-Ni Chen(陈巧妮)
Chin. Phys. B, 2018, 27 (**3**): 037101. DOI: 10.1088/1674-1056/27/3/037101

Quantitative determination of the critical points of Mott metal–insulator transition in strongly correlated systems

Yuekun Niu(牛月坤)[1,†], Yu Ni(倪煜)[2], Jianli Wang(王建利)[3], Leiming Chen(陈雷鸣)[3], Ye Xing(邢晔)[3], Yun Song(宋筠)[4,‡], and Shiping Feng(冯世平)[4,§]

[1] *School of Physical Science and Technology, Inner Mongolia University, Hohhot* 010021, *China*
[2] *College of Physics and Electronic Information, Yunnan Normal University, Kunming* 650500, *China*
[3] *School of Materials Science and Physics, China University of Mining and Technology, Xuzhou* 221116, *China*
[4] *Department of Physics, Beijing Normal University, Beijing* 100875, *China*

(Received 12 September 2023; revised manuscript received 23 October 2023; accepted manuscript online 26 October 2023)

Mottness is at the heart of the essential physics in a strongly correlated system as many novel quantum phenomena occur in the metallic phase near the Mott metal–insulator transition. We investigate the Mott transition in a Hubbard model by using the dynamical mean-field theory and introduce the local quantum state fidelity to depict the Mott metal–insulator transition. The local quantum state fidelity provides a convenient approach to determining the critical point of the Mott transition. Additionally, it presents a consistent description of the two distinct forms of the Mott transition points.

Keywords: critical point, metal–insulator transition, local quantum state fidelity, strongly correlated system, quasiparticle coherent weight

PACS: 71.30.+h, 71.27.+a, 71.10.−w **DOI:** 10.1088/1674-1056/ad0719

1. Introduction

The Mott metal–insulator transition (MIT),[1–3] resulting from the interplay between the kinetic energy t and the on-site Coulomb repulsive interaction U among electrons, represents a fundamental manifestation of strong electron correlation effects. Experimental investigations have demonstrated the presence of the unconventional superconductivity and other exotic quantum phenomena in the metallic phase close to the Mott MIT.[3] This is why the quantitative determination of the critical point of the Mott MIT is crucial to deeply understanding the essential physics of these novel quantum phenomena in strongly correlated systems.

Although enormous efforts have been made at the experimental and theoretical levels to understand the physical origin of the Mott MIT, together with the associated novel quantum phenomena,[3] the quantitative determination of the critical point of the Mott MIT is still a challenging issue. In early studies, it was shown in the Gutzwiller approximation that the quasiparticle coherent weight can be used as a physical quantity to determine the critical point of the Mott MIT, where the quasiparticle coherent weight $Z_{\rm F}$ disappears and the effective mass diverges as $1/Z_{\rm F}$ when the strength of the Coulomb interaction approaches its critical value.[4–6] The quasiparticle coherent peak around the Fermi surface comes mainly from the scattering of electrons on the local-spin fluctuations. Hence, its disappearance at the critical point of MIT can also be tracked by analyzing the energy dependence of the electron self-energy with different Coulomb repulsive interactions.[7] Later, a systematic analysis[8] based on the dynamical mean-field theory (DMFT) indicated that at low-temperature, the opening of the gap and the vanishing of the quasiparticle coherent peak do not happen at the same critical value of $U_{\rm c}$. Instead, MIT is found as a function of U/t, with the corresponding metallic and insulating solutions coexisting between $U_{\rm c2}$ and $U_{\rm c1}$, respectively. Since then, a series of studies focusing on the region of the metallic and insulating solutions coexisting between $U_{\rm c2}$ and $U_{\rm c1}$ has been made.[9–15] In practice, these studies also indicate that the quasiparticle coherent weight $Z_{\rm F}$ may not be able to mark out these two distinct forms of the critical points in the MIT due to the coexistence of a branch of metastable metallic solution that connects the two stable metallic and insulating solutions of $Z_{\rm F}$.[16,17] In this case, a natural question is raised: is there a more proper physical quantity to present the existence of the two distinct forms of the critical points in the Mott MIT?

In this paper, we study the one-band Hubbard model by using the DMFT with the Lanczos method as its impurity solver. It is confirmed that the local quantum state fidelity (LQSF), as a proper physical quantity, can provide a convenient way to identify the critical point of the Mott MIT. In particular, it can give a consistent description of the two different forms of the critical points in the Mott MIT.

[†]Corresponding author. E-mail: ykniu@imu.edu.cn
[‡]Corresponding author. E-mail: yunsong@bnu.edu.cn
[§]Corresponding author. E-mail: spfeng@bnu.edu.cn

© 2024 Chinese Physical Society and IOP Publishing Ltd

2. Models and methods

The one-band Hubbard model is the simplest model that captures the essential physics of MIT in a strongly correlated system. The Hamiltonian of the one-band Hubbard model is given by[18–21]

$$H = -t\sum_{\langle ij\rangle\sigma} d^{\dagger}_{i\sigma}d_{j\sigma} - \mu\sum_{i\sigma} d^{\dagger}_{i\sigma}d_{i\sigma} + \frac{U}{2}\sum_{i\sigma} n_{i\sigma}n_{i\bar{\sigma}}, \tag{1}$$

where the summation $\langle ij\rangle$ is over all sites i, and for each site i, restricted to its nearest-neighbor (NN) sites j, t denotes the electron NN hopping amplitude, U is the on-site Coulomb repulsion between electrons, and μ is the chemical potential. $d^{\dagger}_{i\sigma}$ ($d_{i\sigma}$) is the creation (annihilation) operator for an electron with spin σ at lattice site i, and $n_{i\sigma}$ is the occupation number operator of electrons at lattice site i. Unless explicitly stated, we set $t = 1$ as the energy scale in this paper. The electron Green's function of the Hubbard model (1) can be expressed formally as

$$\mathcal{G}_{\sigma}(\boldsymbol{k},\omega) = \frac{1}{\omega + \mu - \varepsilon_{\boldsymbol{k}} - \Sigma_{\sigma}(\boldsymbol{k},\omega)}, \tag{2}$$

where the energy dispersion in the tight-binding approximation can be obtained directly by $\varepsilon_{\boldsymbol{k}} = \sum_{ij} t_{ij} \mathrm{e}^{\mathrm{i}\boldsymbol{k}\cdot(\boldsymbol{R}_i - \boldsymbol{R}_j)}$, while the effect of interaction in the Hubbard model (1) has been encoded in the electron self-energy $\Sigma_{\sigma}(\boldsymbol{k},\omega)$. It should be emphasized that in the infinite-dimensional system, this electron self-energy $\Sigma_{\sigma}(\boldsymbol{k},\omega)$ is momentum independent. The DMFT[22,23] provides an approximate solution to this electron self-energy $\Sigma_{\sigma}(\boldsymbol{k},\omega)$ in a finite-dimensional system by setting $\Sigma_{\sigma}(\boldsymbol{k},\omega) = \Sigma^{(\mathrm{AIM})}_{\sigma}(\omega)$, where the momentum independence of the electron self-energy $\Sigma^{(\mathrm{AIM})}_{\sigma}(\omega)$ can be obtained in terms of an auxiliary impurity model consisting of a single interacting site in a self-consistently determined bath.[15] In other words, the auxiliary impurity model provides a way to calculate the local electron self-energy $\Sigma^{(\mathrm{AIM})}_{\sigma}(\omega)$ and to use the entire repertoire of the electron Green's function with the contribution to the electron self-energy taken from the auxiliary impurity system rather than from a perturbation expansion.[24]

We evaluate the electron self-energy of the Hubbard model (1) by using the DMFT with the Lanczos method as its impurity solver. In the framework of the DMFT, the Hubbard model (1) is mapped onto an effective single impurity model by dropping the nonlocal contribution to the electron self-energy,

$$\begin{aligned} H_{\mathrm{imp}} =& \sum_{m\sigma}\varepsilon_m c^{\dagger}_{m\sigma}c_{m\sigma} + \sum_{m\sigma} V_m(c^{\dagger}_{m\sigma}d_{\sigma} + d^{\dagger}_{\sigma}c_{m\sigma}) \\ &+ \sum_{\sigma}(\varepsilon - \mu)d^{\dagger}_{\sigma}d_{\sigma} + \frac{U}{2}\sum_{\sigma} n_{d\sigma}n_{d\bar{\sigma}}, \end{aligned} \tag{3}$$

which becomes exact in the limit of the infinite lattice coordination.[25] Here, $d^{\dagger}_{\sigma}$ (d_{σ}) creates (annihilates) a particle in the impurity orbital and $c^{\dagger}_{m\sigma}$ ($c_{m\sigma}$) creates (annihilates) an electron in a conduction band, where the impurity orbital and conduction band are coupled with each other via effective parameters ε_m and V_m, which are determined by the self-consistent DMFT calculation utilizing an impurity solver. In the following discussions, we introduce the local-electron Green's function in real-space as[26,27]

$$\mathcal{G}_{\sigma}(\tau) = -\langle T_{\tau} d_{\sigma}(\tau) d^{\dagger}_{\sigma}(0)\rangle, \tag{4}$$

with the imaginary time $\tau = \mathrm{i}t$. This local-electron Green's function (4) in energy space can be obtained directly by performing the Fourier transformation

$$\mathcal{G}_{\sigma}(\mathrm{i}\omega_n) = \int_0^{\beta} \mathrm{d}\tau\, \mathrm{e}^{\mathrm{i}\omega_n\tau}\mathcal{G}_{\sigma}(\tau), \tag{5}$$

$$\mathcal{G}_{\sigma}(\tau) = \frac{1}{\beta}\sum_{n=-\infty}^{\infty} \mathrm{e}^{-\mathrm{i}\omega_n\tau}\mathcal{G}_{\sigma}(\mathrm{i}\omega_n), \tag{6}$$

where $-\beta \le \tau \le \beta$ and the fermionic Matsubara frequency $\omega_n = (2n+1)\pi/\beta$ with $n = 0, \pm1, \pm2, \ldots$.

The local properties of the Hubbard model on the Bethe lattice can be obtained via a single-site impurity problem supplemented by the following self-consistent relation:[28,29]

$$\mathcal{G}^{-1}_{0\sigma}(\mathrm{i}\omega_n) = \mathrm{i}\omega_n + \mu - t^2\mathcal{G}_{\sigma}(\mathrm{i}\omega_n), \tag{7}$$

where $\mathcal{G}_{0\sigma}$ is the bare Green's function. The self-consistent relation ensures that the on-site (local) component of the Green's function $[\mathcal{G}_{ii}(\mathrm{i}\omega_n) = \frac{1}{N}\sum_k \mathcal{G}(\boldsymbol{k},\mathrm{i}\omega_n)]$ coincides with the Green's function $\mathcal{G}_{\sigma}(\mathrm{i}\omega_n)$ calculated from the effective action.

The Green's function $\mathcal{G}_{\mathrm{imp}}(\mathrm{i}\omega_n)$ of the impurity model (3) is then calculated by the Lanczos method,[30–32] which can be expressed explicitly as[8,28,33]

$$\mathcal{G}_{\mathrm{imp}}(\mathrm{i}\omega_n) = \mathcal{G}^{+}_{\sigma}(\mathrm{i}\omega_n) + \mathcal{G}^{-}_{\sigma}(\mathrm{i}\omega_n), \tag{8}$$

with $\mathcal{G}^{+}_{\sigma}(\mathrm{i}\omega_n)$ and $\mathcal{G}^{-}_{\sigma}(\mathrm{i}\omega_n)$ given by

$$\mathcal{G}^{+}_{\sigma}(\mathrm{i}\omega_n) = \cfrac{\langle\phi_0|d_{\sigma}d^{\dagger}_{\sigma}|\phi_0\rangle}{\mathrm{i}\omega_n - a^{(+)}_0 - \cfrac{b^{(+)2}_1}{\mathrm{i}\omega_n - a^{(+)}_1 - \cfrac{b^{(+)2}_2}{\mathrm{i}\omega_n - a^{(+)}_2 - \cdots}}}, \tag{9}$$

$$\mathcal{G}^{-}_{\sigma}(\mathrm{i}\omega_n) = \cfrac{\langle\phi_0|d^{\dagger}_{\sigma}d_{\sigma}|\phi_0\rangle}{\mathrm{i}\omega_n + a^{(-)}_0 - \cfrac{b^{(-)2}_1}{\mathrm{i}\omega_n + a^{(-)}_1 - \cfrac{b^{(-)2}_2}{\mathrm{i}\omega_n + a^{(-)}_2 - \cdots}}}, \tag{10}$$

where a_n (b_n) is the nth sub-diagonal element of the tridiagonalized Hamiltonian obtained by the Lanczos method and $|\phi_0\rangle$ is the ground state of the Hamiltonian (3). In our calculations, we choose $n_{\mathrm{b}} = 7$ and $\beta = 1024$ to assure the accuracy of the self-consistency calculations, especially in the low-energy region. It is worth noting that β plays a role of

frequency cutoff,[28] and hence $1/\beta$ can be regarded as a fictitious temperature. In this work, we restrict our calculations to zero-temperature conditions.

The Green's function behaves differently depending on whether the eigenstates are localized or extended,[34] which helps us to obtain the interaction effect on the phase transitions. For an interaction-driven Mott transition, the ground state of the metallic phase is gapless, while the Mott insulating ground state has a gap. As discussed in Refs. [35–38], there is a short-range entanglement in gapped quantum states, which corresponds to a symmetry-protected topological (SPT) order.[37] We extend the classification method of the SPT phases in higher dimensions to label-gapped quantum phases based on the four occupation states of electrons on an impurity site. Additionally, the fidelity per site method[39,40] is in accord with the DMFT idea of mapping a lattice model onto an effective single-site impurity model.[8] It has been demonstrated that the fidelity per site method can help us understand how quantum phase transitions are influenced by quantum fluctuations.[39,40] Considering the scenario of the SPT[35–38,41,42] and the sensitive feature of fidelity in detecting quantum fluctuation,[40] we introduce the local quantum state fidelity[43] of single impurity site as

$$L_{\rm o} = -\frac{1}{\beta}\sum_{n=-\infty}^{\infty} {\rm e}^{{\rm i}\omega_n 0^+}\mathcal{G}_{\rm imp}({\rm i}\omega_n)\langle\Phi^{\rm o}_{\rm imp}|\hat{P}|\Phi^{\rm o'}_{\rm imp}\rangle, \tag{11}$$

with

$$|\Phi^{\rm o}_{\rm imp}\rangle = \sum_{s=1}^{4} p_s|p_s\rangle = p_1|0\rangle + p_2|\uparrow\rangle + p_3|\downarrow\rangle + p_4|\uparrow\downarrow\rangle.$$

Here, $\hat{P}$ is the net spin projection operator for impurity site with $\langle 0|\hat{P}|0\rangle = \langle\uparrow\downarrow|\hat{P}|\uparrow\downarrow\rangle = 0$, $\langle\uparrow|\hat{P}|\uparrow\rangle = 1$, and $\langle\downarrow|\hat{P}|\downarrow\rangle = -1$. $|\Phi^{\rm o}_{\rm imp}\rangle$ ($|\Phi^{\rm o'}_{\rm imp}\rangle$) represents the ground state wave function of the single impurity site with an interaction strength of U ($U+0^+$). The factor ${\rm e}^{{\rm i}\omega_n 0^+}$ is introduced to ensure the convergence of the summations.

In the metallic phase, the average spin of the DMFT impurity $\langle\sigma\rangle_t$ is zero[44] because of the high symmetry of the spin at the impurity site obtained by Landau's theory. The probabilities of doublon and holon[45] occurrence are equal, i.e., $p_1^2 = p_4^2$, and the probabilities of spin-up and spin-down states have $p_2^2 = p_3^2$, and therefore the LQSF remains zero ($L_{\rm o} = 0$). However, the insulating ground state of the DMFT impurity model is double-degenerate with singly occupied states of opposite spins ($|\uparrow\rangle$ or $|\downarrow\rangle$), and thus $L_{\rm o}$ has two solutions as $L_{\rm o} = \pm C$, where C is a finite positive constant. Because both the positive and negative signs of $L_{\rm o}$ indicate the same insulating phase, we only show the absolute value of $L_{\rm o}$ in the figures. As a result, a sudden rise of the LQSF at the critical interaction $U_{\rm c}$ will be found (note that $L_{\rm o} = \pm C$ does not mean that the system is antiferromagnetic or ferromagnetic). Specifically, the local moment of the impurity site is zero due to the double degeneration of the ground state. Therefore, the Mott MIT can be depicted by the LQSF. It is worth noticing that the behavior of $L_{\rm o}$ is the same as the topological invariant found in Ref. [46].

To evaluate the frequency summation over the Matsubara Green's function, we need to further simplify the above formula by considering the interacting Matsubara Green's function at the poles, which holds

$$[\mathcal{G}_\sigma({\rm i}\omega_n)] = [\mathcal{G}_\sigma(-{\rm i}\omega_n)]^*,$$
$$\omega_n = \frac{(2n+1)\pi}{\beta},\ \ n = 0,1,2,\ldots. \tag{12}$$

With the help of the above Eq. (12), the LQSF of the impurity site can be rewritten explicitly as $L_{\rm o} = -(2/\beta){\rm Re}\sum_{n=0}^{\infty}{\rm e}^{{\rm i}\omega_n 0^+}\mathcal{G}_{\rm imp}({\rm i}\omega_n)\langle\Phi^{\rm o}_{\rm imp}|\hat{P}|\Phi^{\rm o}_{\rm imp}\rangle$, indicating that $L_{\rm o}$ can be directly obtained by a summation of the positive frequencies in the effective on-site problem.

3. Results

We define the quasiparticle coherent weight $Z_{\rm F}$ as[27,47]

$$\frac{1}{Z_{\rm F}} = 1 - \frac{\partial}{\partial\omega}{\rm Re}\Sigma_\sigma(\omega)|_{\omega=0} \approx 1 - \frac{{\rm Im}\Sigma_\sigma({\rm i}\omega_0)}{\omega_0}, \tag{13}$$

where the local self-energy $\Sigma_\sigma({\rm i}\omega_n)$ is obtained from the local Green's function in Eq. (7). In the following discussions, we study the Mott MIT of the Hubbard model at half-filling in terms of the evolution of the LQSF $L_{\rm o}$ at the impurity site with the on-site Coulomb repulsive interaction U. In Fig. 1 we plot $2L_{\rm o}$ as a function of interaction U, where the red dashed-line indicates the position of the critical point of the Mott MIT. For a better comparison, the evolution of the quasiparticle coherent weight $Z_{\rm F}$ (blue solid-line) with U is also presented in Fig. 1. $Z_{\rm F}$ usually decreases with increasing U and keeps very close to zero when approaching the critical interaction $U_{\rm c}$ of the Mott MIT, near which the systematic errors of $Z_{\rm F}$ increase significantly, leading to difficulties in the quantitative determination of the critical point of MIT. More crucially, within the framework of DMFT, two metallic results with different slope ${\rm d}Z_{\rm F}/{\rm d}U$ are found to coexist in a finite range of interaction strengths,[16,17] and thus comparing the respective energies with the energy of the insulator is suggested.[17] Consequently, it becomes quite difficult and inconvenient to numerically determine the actual critical interaction $U_{\rm c}$ by the quasiparticle coherent weight. In a striking contrast to the complex of $Z_{\rm F}$ that has two metallic solutions in the coexistence region of interaction U, the LQSF $L_{\rm o}$ keeps equal to zero for both the metastable and stable metallic solutions when $U < U_{\rm c}$, as shown in Fig. 1.

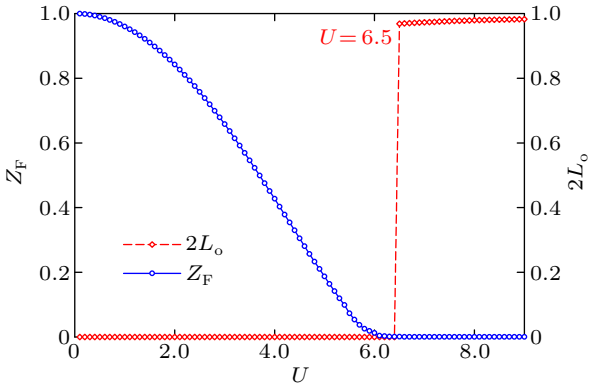


Fig. 1. The local quantum state fidelity L_o (red dotted line) as a function of interaction U. The Mott metal–insulator transition occurs at a critical value of $U_c = 6.5$. For comparison, the evolution of the quasiparticle coherent weight Z_F with U (blue solid line) is also presented. In the numerical calculations we chose $n_b = 7$ and $\beta = 1024$.

However, at the critical point $U_c = 6.5$ of MIT, the LQSF jumps abruptly from $L_o = 0$ in the metallic phase to $2L_o \approx 1.0$ in the insulating phase. Our results indicate clearly that the LQSF L_o at the impurity site is very sensitive to the existence of the resonant peak at the Fermi level, which therefore is a more proper physical quantity to quantitatively depict the critical point of the Mott MIT.

As to the two classes of solutions, (i) the solution from the metallic phase towards the critical interaction of MIT (the metallic-phase solution U_{c2}) and (ii) the solution from the insulating phase towards the critical point of MIT (the insulating-phase solution U_{c1}), the LQSF L_o as a more proper physical quantity of MIT can give a natural explanation of the difference between the metallic and insulating solutions. In this case, we have made a series of calculations for $2L_o$, and the results of the metallic solution of $2L_o$ (red dotted line) and the insulating solution (blue solid line) are plotted in Fig. 2, where $U_{c1} = 4.7$ and $U_{c2} = 6.5$ are the critical points of the insulator-to-metal transition and the metal-to-insulator transition, respectively. Our findings of the critical interactions are in agreement with the DMFT results from the numerical renormalization group solver[5] $U_{c1} = 5.0$ and $U_{c2} = 5.88$, and the dynamical density renormalization group method[48] $U_{c1} = 4,76$ and $U_{c2} = 6.14$. The results in Fig. 2 show that apart from a metallic phase in the weak interaction region ($U < U_{c1}$) and an insulating phase in the strong interaction region ($U > U_{c2}$), there is an intermediate interaction region ($U_{c1} < U < U_{c2}$), where the metallic solution coexists with the insulating solution. Within this intermediate interaction region, $2L_o$ as a function of U exhibits a hysteretic behavior since both the metallic and insulating solutions are found to be attractive points of a particle–hole symmetry system.[15] The results in Figs. 1 and 2 therefore show that L_o is a more proper physical parameter to give a quantitative description of the Mott MIT in a strong correlation system.

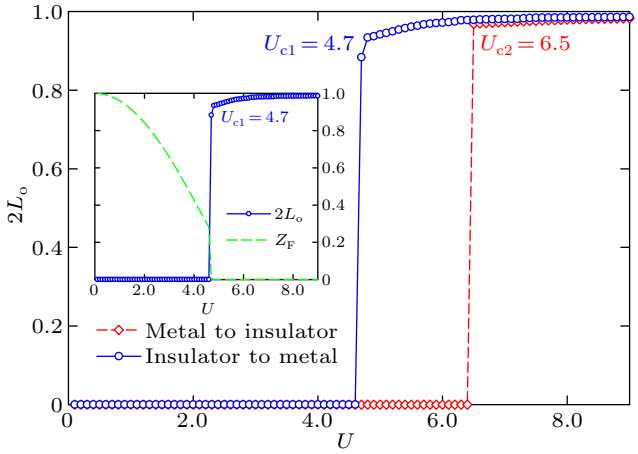


Fig. 2. The local quantum state fidelity L_o as a function of interaction U. The blue line indicates the critical point at $U_{c1} = 4.7$, while the red line denotes the critical point at $U_{c2} = 6.5$. Within the region between the two critical points of U_{c_1} and U_{c2}, the insulating solution (blue solid line) and metallic solution (red dotted line) coexist. Inset: the comparison of the local quantum state fidelity (blue solid line) and the quasiparticle coherent weight (green dotted line) for the insulating-phase solution.

Although the summation of Matsubara frequency is from zero to infinity, the actual calculation is performed numerically with the infinitude of Matsubara frequency $n = 0, 1, 2, \ldots, \infty \to n = 0, 1, 2, \ldots, n_{max}$ replaced by a finite n_{max}. In this case, we have made a series of calculations for $2L_o$ as a function of U at different cutoff n_{max}, and the results are plotted in Fig. 3, where the critical points at $n_{max} = 2048$, $n_{max} = 8192$, $n_{max} = 32768$ and $n_{max} = 65536$ are very close to each other, indicating that for the large enough n_{max}, the error bars are small enough. In particular, U_c can be extrapolated as $U_c = 6.5$ in the case of $n_{max} = \infty$.

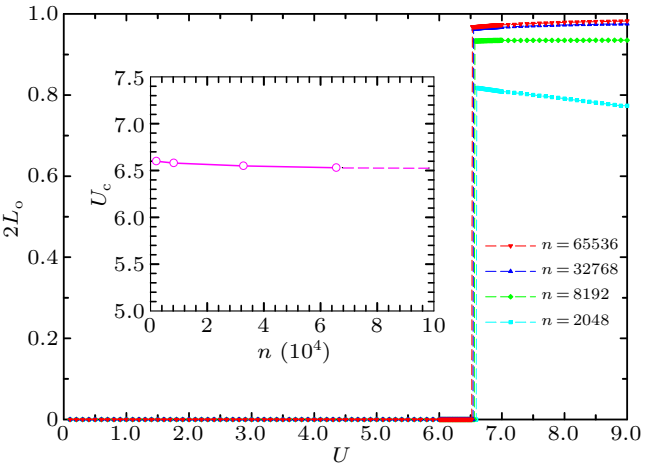


Fig. 3. The local quantum state fidelity L_o as a function of the interaction U for various cutoff values n in the series summation. The evolution of U_c with n (circles) is presented (inset) along with the fitting line (solid line) and its extension (dashed line).

The Hilbert space of each site in the Hubbard model (1) consists of four states, $|0\rangle$, $|\uparrow\rangle$, $|\downarrow\rangle$, $|\uparrow\downarrow\rangle$, corresponding to the zero, spin-up, spin-down and double-electron-occupied states, respectively. The probabilities of the zero, spin-up, spin-down and double-occupied states at the single impurity site of the metallic solution are plotted in Fig. 4, which shows clearly

that the probabilities of the zero and double-occupied states are equal and decrease simultaneously in the metallic phase. However, the probability of the spin-up singly occupied state increases with the increase of the on-site Coulomb interaction U and jumps to $p^2 \approx 1$ at the critical point $U_{c2} = 6.5$. The same feature for the probability of the spin-down singly occupied state is found in the insulating phase due to the degeneration (see Fig. 4 inset). Concomitantly, the LQSF is equal to zero when the probability of the spin-up singly occupied state is equal to that of the spin-down singly occupied state in the metallic phase. However, in a striking contrast to the case in the metallic phase, the feature of the probability of the spin-up singly occupied state is quite different from that of the probability of the spin-down singly occupied state in the insulating phase, and a jump of the LQSF is found at the critical point due to the presence of two degenerate solutions with opposite spin occupancies. The above results correspond to the theoretical prediction of Eq. (11). This is why the LQSF in Eq. (11) is a more proper physical quantity to give a quantitative depiction of two distinct forms of the critical points in the MIT of a strongly correlated system.

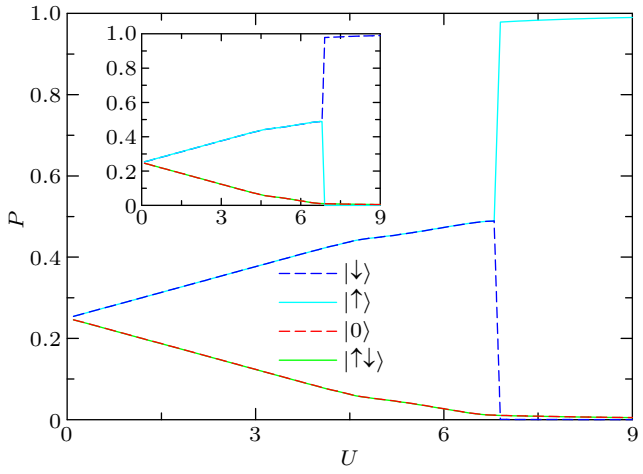


Fig. 4. The probabilities p^2 of the zero-occupied state $|0\rangle$ (red dashed line), spin-up occupied state $|\uparrow\rangle$ (cyan solid line), spin-down occupied state $|\downarrow\rangle$ (blue dashed line) and double-occupied state $|\uparrow\downarrow\rangle$ (green solid line) in the impurity ground state as a function of the interaction U. Inset: another solution with opposite p^2 of the spin-up and spin-down occupied states when $U > U_c$, demonstrating the double-degeneration of the ground state within the insulating phase.

4. Conclusions

Based on the one-band Hubbard model, we have studied the Mott MIT in a strongly correlated system by using the combined approach of the DMFT and the Lanczos technique. Our results clearly demonstrate that the LQSF serves as a proper physical quantity for depicting the Mott MIT in a strongly correlated system. It allows for quantitative determination of the critical points and provides a consistent description of two distinct forms of the critical points. The LQSF can be also used to discuss the novel physics in orbital-selective Mott insulators[49] and superconductors.[50,51] In particular, it may be applied to explain the hysteresis observed experimentally in Mott-field effect transistors.[52] These related works are currently under study.

Acknowledgments

The authors would like to thank Gabriele Bellomia for fruitful discussions. YN is also grateful to Louk Rademaker and Haiming Dong for helpful discussions. Project supported by the Scientific Research Foundation for Youth Academic Talent of Inner Mongolia University (Grant No. 10000-23112101/010) and the Fundamental Research Funds for the Central Universities of China (Grant No. JN200208). YS is supported by the National Natural Science Foundation of China (Grant No. 11474023). SF is supported by the National Key Research and Development Program of China (Grant No. 2021YFA1401803) and the National Natural Science Foundation of China (Grant Nos. 11974051 and 11734002).

References

[1] Mott N F 1949 *Proc. Phys. Soc. Sect. A* **62** 416
[2] Mott N F 1968 *Rev. Mod. Phys.* **40** 677
[3] Imada M, Fujimori A and Tokura Y 1998 *Rev. Mod. Phys.* **70** 1039
[4] Brinkman W F and Rice T M 1970 *Phys. Rev. B* **2** 4302
[5] Bulla R 1999 *Phys. Rev. Lett.* **83** 136
[6] Bulla R and Potthoff M 2000 *Eur. Phys. J. B* **13** 257
[7] Turkowski V 2021 *Dynamical Mean-Field Theory for Strongly Correlated Materials* (Switzerland: Springer Cham) pp. 41–130
[8] Georges A, Kotliar G, Krauth W and Rozenberg M J 1996 *Rev. Mod. Phys.* **68** 13
[9] Florens S, Georges A, Kotliar G and Parcollet O 2022 *Phys. Rev. B* **66** 205102
[10] Feldbacher M, Held K and Assaad F F 2004 *Phys. Rev. Lett.* **93** 136405
[11] Raas C and Uhrig G S 2009 *Phys. Rev. B* **79** 115136
[12] Sordi G, Haule K and Tremblay A M S 2011 *Phys. Rev. B* **84** 075161
[13] Eisenlohr G, Lee S S B and Vojta M 2019 *Phys. Rev. B* **100** 155152
[14] Zhou S, Liang L and Wang Z 2020 *Phys. Rev. B* **101** 035106
[15] van Loon E G C P, Krien F and Katanin A A 2020 *Phys. Rev. Lett.* **125** 136402
[16] Chatzieleftheriou M, Kowalski A, Berovic M, Amaricci A, Capone M, De Leo L, Sangiovanni G and de'Medici L 2023 *Phys. Rev. Lett.* **130** 066401
[17] Ono Y, Potthoff M and Bulla R 2003 *Phys. Rev. B* **67** 035119
[18] Kanamori J 1963 *Progress of Theoretical Physics* **30** 275
[19] Hubbard J 1963 *P. Roy. Soc. Lond. A* **276** 238
[20] Hubbard J 1964 *P. Roy. Soc. Lond. A* **277** 237
[21] Hubbard J 1964 *P. Roy. Soc. Lond. A* **281** 401
[22] Muller-Hartmann E 1989 *Z. Phys. B* **74** 507
[23] Metzner W and Vollhardt D 1989 *Phys. Rev. Lett.* **62** 324
[24] Richard M M, Lucia R and David M C 2016 *Interacting Electrons: Theory and computational approach* (Cambridge: Cambridge University Press) pp. 421-456
[25] Georges A and Kotliar G 1992 *Phys. Rev. B* **45** 6479
[26] Anisimov V and Izyumov Y 2010 *Electronic Structure of Strongly Correlated Materials* (Heidelberg: Springer Berlin) pp. 47–120
[27] Mahan G D 2000 *Many-Particle Physics* (New York: Springer New York) pp. 81–238
[28] Caffarel M and Krauth W 1994 *Phys. Rev. Lett.* **72** 1545
[29] Laloux L, Georges A and Krauth W 1994 *Phys. Rev. B* **50** 3092
[30] Dagotto E 1994 *Rev. Mod. Phys.* **66** 763
[31] Niu Y K, Sun J, Ni Y, Liu J Y, Song Y and Feng S P 2019 *Phys. Rev. B* **100** 075158
[32] Amaricci A, Crippa L, Scazzola A, Petocchi F, Mazza G, de'Medici L and Capone M 2022 *Computer Physics Communications* **273** 108261
[33] Capone M, de'Medici L and Georges A 2007 *Phys. Rev. B* **76** 245116

[34] Economou E N 2006 *Green's Functions in Quantum Physics* (Heidelberg: Springer Berlin) pp. 249–283

[35] Gu Z C and Wen X G 2009 *Phys. Rev. B* **80** 155131

[36] Chen X, Gu Z C and Wen X G 2010 *Phys. Rev. B* **82** 155138

[37] Lan T, Kong L and Wen X G 2017 *Phys. Rev. B* **95** 235140

[38] Chen X, Gu Z C and Wen X G 2011 *Phys. Rev. B* **83** 035107

[39] Zhou H Q and Orús R and Vidal G 2008 *Phys. Rev. Lett.* **100** 080601

[40] Gu S J 2010 *International Journal of Modern Physics B* **24** 4371

[41] Chen Y A, Kapustin A, Turzillo A and You M 2019 *Phys. Rev. B* **100** 195128

[42] Wen X G 2019 *Phys. Rev. B* **99** 205139

[43] Rams M and Damski B 2011 *Phys. Rev. Lett.* **106** 055701

[44] Feng D and Jin G J 2013 *Introduction to Condensed Matter Physics* (Volume I) (Singapore: World Scientific Publishing Co. Pte. Ltd.) pp. 403–419

[45] Yuta M, Martin E and Philipp W 2018 *Phys. Rev. Lett.* **121** 057405

[46] Sen S, Wong P J and Mitchell A K 2020 *Phys. Rev. B* **102** 081110

[47] Perroni C A, Ishida H and Liebsch A 2007 *Phys. Rev. B* **75** 045125

[48] Karski M, Raas C and Uhrig G S 2005 *Phys. Rev. B* **72** 113110

[49] Kotliar G, Savrasov S Y, Haule K, Oudovenko V S, Parcollet O and Marianetti C A 2006 *Rev. Mod. Phys.* **78** 865

[50] Lee P A, Nagaosa N and Wen X G 2006 *Rev. Mod. Phys.* **78** 17

[51] Castro Neto A H, Guinea F, Peres N M R, Novoselov KS and Geim A K 2009 *Rev. Mod. Phys.* **81** 109

[52] Kim H T, Chae B G, Youn D H, Maeng S L, Kim K, Kang K Y and Lim Y S 2004 *New J. Phys.* **6** 52